

Clinical and molecular significance of homologous recombination deficiency positive non-small cell lung cancer in Chinese population: An integrated genomic and transcriptional analysis

Yifei Wang¹, Yidan Ma¹, Lei He¹, Jun Du¹, Xiaoguang Li², Peng Jiao³, Xiaonan Wu⁴, Xiaomao Xu⁵, Wei Zhou⁵, Li Yang¹, Jing Di¹, Changbin Zhu⁶, Liming Xu⁶, Tianlin Sun⁶, Lin Li⁴, Dongge Liu¹, Zheng Wang¹

¹Department of Pathology; ²Department of Minimally Invasive Tumor Therapies Center; ³Department of Thoracic Surgery; ⁴Department of Oncology; ⁵Department of Respiratory and Critical Care Medicine, Beijing Hospital, National Center of Gerontology, Institute of Geriatric Medicine, Chinese Academy of Medical Sciences, Beijing 100730, China; ⁶Amoy Diagnostics Co., Ltd., Xiamen 361027, China

Correspondence to: Zheng Wang. Department of Pathology, Beijing Hospital, No. 1 Dahua Road, Beijing 100730, China. Email: wangzhengmay@163.com; Dongge Liu. Department of Pathology, Beijing Hospital, No. 1 Da Hua Road, Beijing 100730, China. Email: 13661275182@163.com; Lin Li. Department of Oncology, Beijing Hospital, No. 1 Dahua Road, Beijing 100730, China. Email: lilin_51@hotmail.com.

Abstract

Objective: The clinical significance of homologous recombination deficiency (HRD) in breast cancer, ovarian cancer, and prostate cancer has been established, but the value of HRD in non-small cell lung cancer (NSCLC) has not been fully investigated. This study aimed to systematically analyze the HRD status of untreated NSCLC and its relationship with patient prognosis to further guide clinical care.

Methods: A total of 355 treatment-naïve NSCLC patients were retrospectively enrolled. HRD status was assessed using the AmoyDx Genomic Scar Score (GSS), with a score of ≥ 50 considered HRD-positive. Genomic, transcriptomic, tumor microenvironmental characteristics and prognosis between HRD-positive and HRD-negative patients were analyzed.

Results: Of the patients, 25.1% (89/355) were HRD-positive. Compared to HRD-negative patients, HRD-positive patients had more somatic pathogenic homologous recombination repair (HRR) mutations, higher tumor mutation burden (TMB) ($P < 0.001$), and fewer driver gene mutations ($P < 0.001$). Furthermore, HRD-positive NSCLC had more amplifications in PI3K pathway and cell cycle genes, *MET* and *MYC* in epidermal growth factor receptor (*EGFR*)/anaplastic lymphoma kinase (*ALK*) mutant NSCLC, and more *PIK3CA* and *AURKA* in *EGFR/ALK* wild-type NSCLC. HRD-positive NSCLC displayed higher tumor proliferation and immunosuppression activity. HRD-negative NSCLC showed activated signatures of major histocompatibility complex (MHC)-II, interferon (IFN)- γ and effector memory CD8⁺ T cells. HRD-positive patients had a worse prognosis and shorter progression-free survival (PFS) to targeted therapy (first- and third-generation EGFR-TKIs) ($P = 0.042$). Additionally, HRD-positive, *EGFR/ALK* wild-type patients showed a numerically lower response to platinum-free immunotherapy regimens.

Conclusions: Unique genomic and transcriptional characteristics were found in HRD-positive NSCLC. Poor prognosis and poor response to EGFR-TKIs and immunotherapy were observed in HRD-positive NSCLC. This study highlights potential actionable alterations in HRD-positive NSCLC, suggesting possible combinational therapeutic strategies for these patients.

Keywords: Non-small cell lung cancer; homologous recombination deficiency; genetic alterations; transcriptional analysis; tumor microenvironment; prognosis

Submitted Apr 10, 2024. Accepted for publication Jun 20, 2024.

doi: 10.21147/j.issn.1000-9604.2024.03.05

View this article at: <https://doi.org/10.21147/j.issn.1000-9604.2024.03.05>

Introduction

Non-small cell lung cancer (NSCLC) accounts for about 85% of all lung cancers (1). Approximately 80% of these cases are diagnosed at stage III or IV and are primarily treated with systemic therapies such as chemotherapy, immunotherapy, or targeted agents (2,3). While targeted therapies are feasible for patients with molecular alterations, drug resistance is inevitable (4). Less than 20% of unscreened NSCLC patients respond to immunotherapy, and some develop severe immunotoxicity (5). Platinum-based chemotherapy remains a cornerstone of NSCLC treatment (6). Given the advances in molecular characterization of lung cancer, new targeted therapies for NSCLC are being investigated (7). Therefore, it is critical to identify predictive markers for NSCLC therapy to improve treatment outcomes and prolong patient survival.

Homologous recombination repair (HRR), a sub-process of DNA double-strand break repair (DDR), is often defective in cancer, leading to DNA damage accumulation and genomic instability, known as homologous recombination deficiency (HRD). Many new cancer therapies under development target the DDR pathway, particularly homologous recombination gene inhibitors, such as poly (adenosine diphosphate-ribose) polymerase (PARP) inhibitors, which harness the synthetic lethality of HRD (8). Therefore, HRD scoring algorithms have been developed using different detection methods to quantify the degree of genomic instability (9-11). The clinical value of HRD score has been established in breast, ovarian and prostate cancers. However, the percentage of lung cancers with HRD is currently undefined, and research on the role of HRD score as a biomarker for response to different therapies in NSCLC is still ongoing.

Pan-cancer analyses revealed that bi-allelic inactivation of HR pathway genes occurs in over 5% of all cancers, including NSCLC (12). Shim *et al.* identified HRD in 18.7% of patients with advanced NSCLC (13). In another study using the Foundation Medicine LOH/HRD genomic score, HRD was found in 66% of patients (14). Data analysis from The Cancer Genome Atlas (TCGA) showed that over one-third of NSCLC patients were HRD score positive, with differences in mutation profiles between high-HRD and low-HRD score patients (15). Notably,

high-HRD score patients had alterations in tumor suppressor genes such as *TP53*, *LRP1B* and *CDKN2A*, whereas low-HRD score patients had more *KRAS* and *ERBB2* mutations (16).

Several clinical (17-19) and preclinical (20) studies have shown a correlation between HRD status and therapy efficacy and prognosis in NSCLC. Analysis based on the TCGA database indicated that high-HRD score patients had a worse prognosis and poorer response to immunotherapy compared to low-HRD score patients (21). However, results from Zhou *et al.* showed that HR pathway mutations might enhance the efficacy of immunoneoadjuvant therapy for NSCLC (17). A clinical trial (PIN trial) in advanced, unscreened NSCLC patients showed no significant benefit from PARP inhibitor (PARPi) as maintenance therapy (18). Ongoing clinical trials, such as the Lung-MAP SWOG S1400G trial (No. NCT02154490), are observing the effect of *BRCA* gene mutation or HRD status on PARPi combination therapy. Additionally, the impact of HRD status on the efficacy of targeted therapy and platinum-based chemotherapy is seldom reported, though evidence suggests HR gene mutations might predict sensitivity to platinum-based chemotherapy in advanced NSCLC (19). No current studies appear to have systematically investigated the genomic and transcriptional significance of untreated NSCLC patients with different HRD statuses.

In this study, we collected treatment-naïve NSCLC samples to explore the prognostic value of HRD status in advanced NSCLC therapies. Comprehensive genomic profiling of 571 cancer-related genes and targeted RNA sequencing for 2,660 onco-immunology genes were conducted. By integrating molecular profiling data and clinicopathological features, we analyzed factors affecting prognosis. This determined the biological and clinical significance of HRD status in NSCLC to further guide clinical diagnosis and treatment.

Materials and methods

Patients and clinical data collection

This study retrospectively screened 447 NSCLC patients with clinical pathology and HRD detection records at

Beijing Hospital from July 2019 to April 2023. Eligibility criteria included: 1) patients pathologically diagnosed with NSCLC; 2) patients who had not received second-line or post-second-line therapy; and 3) patients with HRD detection records. Finally, 355 NSCLC patients met these criteria and were enrolled in the study. Clinicopathological information, including age, gender, family history, smoking history, tumor-node-metastasis (TNM) stage, molecular detection results of tissue, and treatment history, was collected from the clinical case and pathological information systems of Beijing Hospital (Figure 1). Survival follow-up data were analyzed using an October 30, 2023, data cut-off. The study was approved by the Human Ethics Committee of Beijing Hospital (No: 2023BJYYEC-389-02) with a waiver of the informed consent.

DNA and RNA extraction, library construction and sequencing

The processes for DNA and RNA extraction, library construction, and sequencing were described in previous

literature with minor modifications (22,23). Genomic DNA and RNA were extracted from formalin-fixed paraffin-embedded (FFPE) tumor samples using the AmoyDx FFPE DNA/RNA Kit (Cat.#8.02.23501X036G/8.02.24101X036G, AmoyDx, Xiamen, China). DNA and RNA concentrations were measured using a Quantus fluorometer and dsDNA/RNA HS Assay Kit (Cat.#E2670/E3310, Promega, Madison, USA). Fragment length was assessed using an Agilent 2100 Bioanalyzer and DNA/RNA HS Kit (Cat.#5067-1504/5067-1511, Agilent, Santa Clara, USA). The sequencing library, comprising a panel of 571 genes for DNA mutations and genomic signatures detection [single nucleotide variation (SNV), insertion/deletion (Indel), fusion, copy number variation (CNV), microsatellite instability (MSI), and tumor mutation burden (TMB)] and 2,660 genes for RNA expression and fusion detection, was created using the AmoyDx® Master Panel (Cat.#8.06.0130, AmoyDx) according to the recommended protocol. Sequencing was performed on an Illumina NovaSeq 6000 instrument (Illumina, San Diego, USA).

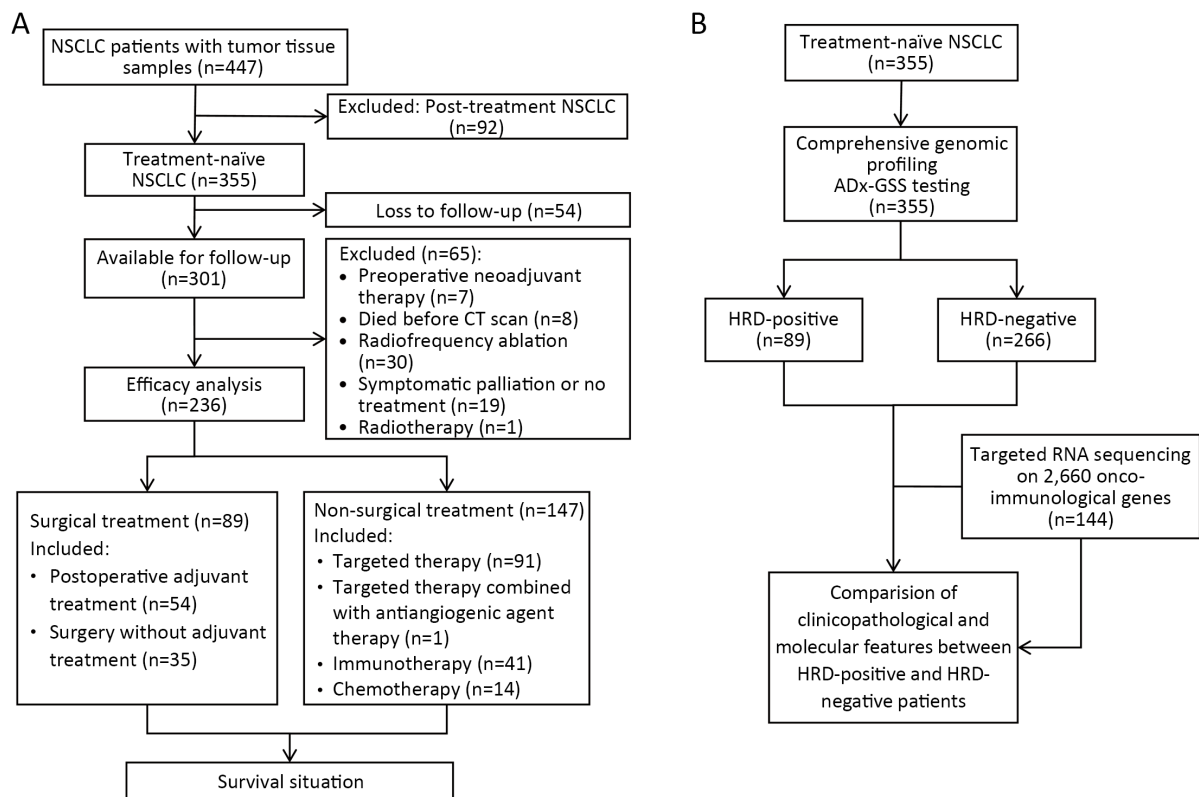


Figure 1 Flowcharts of study design. (A) Flowchart of DNA and RNA next generation sequencing and clinicopathological and molecular features analysis in 355 NSCLC patients; (B) Treatment and prognostic analysis of enrolled NSCLC patients. NSCLC, non-small cell lung cancer; CT, computed tomography; GSS, genomic scar score; HRD, homologous recombination defect.

Mutation calling, filtering and data analysis

Sequencing data were first cleaned to remove sequencing adaptors, low-quality reads (quality<15), or poly-N using Trimmomatic, and then aligned to the human reference genome (hg19) using the BWA-MEM aligner with default parameters (<http://bio-bwa.sourceforge.net/>). Quality control metrics, such as average sequence depth, capture efficiency, duplication rate, alignment rate, coverage, and uniformity of the processed data, were corrected using unique molecular identifiers (UMIs). Synonymous mutations were excluded from analyses. Polymerase chain reaction (PCR) duplicates were removed using MarkDuplicates from the Genome Analysis Toolkit (GATK4, v.4.0.2.1; <https://software.broadinstitute.org/gatk/>). Base Quality Score Recalibration was performed using GATK's Base Recalibrator and ApplyBQSR. After correction, a BAM file was obtained. Non-synonymous SNVs and Indels were called by VarScan2 and HaplotypeCaller/UnifiedGenotyper of GATK to obtain the final VCF files. Fusions were identified by FusionAnnotator/SID Filter (<https://github.com/FusionFilter>). Analysis of variance was used to annotate the VCF files. SNVs and Indels were further filtered using the following criteria: 1) minimum ≥ 5 variant supporting reads and $\geq 1\%$ variant allele frequency; 2) filtered if present in $>2\%$ population frequency in the 1000 Genome Project and GnomAD database; 3) filtered if variants not located in the CDS region; and 4) filtered if not annotated as (likely/predicted) oncogenic in the OncoKB database. Germline variants were called by pairing normal tissue or blood samples. Germline variants were filtered using the following criteria: 1) $\geq 20\%$ variant allele frequency; 2) filtered if present in $>2\%$ population frequency in the 1000 Genome Project and GnomAD database; and 3) variants were classified into five categories according to the American College of Medical Genetics (ACMG) recommendations: class 1, benign; class 2, likely benign; class 3, variant of unknown significance (VUS); class 4, likely pathogenic; and class 5, pathogenic (24). Individuals with likely pathogenic or pathogenic variants were defined as having "pathogenic" variants. The CNV profiles, cellular purity, and ploidy were detected by Sequenza (2.1.2; <http://www.cbs.dtu.dk/biotools/sequenza/>) with default parameters.

HRD status evaluation

HRD status was assessed using the Genomic Scar Score

(GSS) model (25) from AmoyDx by considering the length, type and location of genome-wide chromosomal CNV through 24,000 single nucleotide polymorphisms (SNPs) distributed across the human genome. The GSS was calculated by summing loss of heterozygosity (LOH), large-scale state transition (LST), and telomeric allelic imbalance (TAI) using ANDAS software (Amoy Diagnostics, Xiamen, China). HRD-positive was defined as a $GSS \geq 50$.

Differential expression and pathway analysis

The Wilcoxon rank-sum test, a classical non-parametric statistical test, was used to compare gene expression levels between two conditions (26). Differentially expressed genes (DEGs) were identified based on the following criteria: genes with a fold change of ≥ 1.5 and a P value of < 0.05 for the comparison between HRD-positive and HRD-negative groups. Enrichment analyses were conducted using the R package "clusterProfiler" (27) to determine the functional roles of DEGs. These analyses included Gene Ontology (GO), Kyoto Encyclopedia of Genes and Genomes (KEGG), Hallmark, Wikipathway, and Reactome. Gene Set Enrichment Analysis (GSEA) (28) was also performed using the R package "GSEA".

Tumor microenvironment (TME) evaluation

The Gene Set Variation Analysis (GSVA) algorithm was used to evaluate the relative abundance of infiltrating immune cells in the TME of NSCLC (29). Gene sets for TME-infiltrating immune cells were extracted from previous datasets (30,31). Enrichment scores calculated using the R package "GSVA" were used to determine the relative abundance of each TME-infiltrating cell in NSCLC (32). The deconvolution method CIBERSORT (33) and marker-based approaches MCP-counter (34) were also used to assess the TME.

Statistical analysis

Statistical analyses were conducted using SPSS Statistics (Version 26.0; IBM Corp., New York, USA) and R Project (Version 4.1.2; <https://www.r-project.org/>). The clinicopathological characteristics of the patients were summarized as frequencies (percentages) or medians (quartiles). Chi-square or Fisher's exact tests were used to compare rates or percentages for significance. Non-parametric Wilcoxon rank-sum tests were utilized to

compare medians between two datasets. Univariate Cox proportional hazards regression was used to assess prognostic values using the “survival” R package. Disease-free survival (DFS) and progression-free survival (PFS) were estimated using the Kaplan-Meier method and compared between cohorts or subgroups using a two-sided log-rank test. For all calculations, the tests were two-sided, and $P < 0.05$ was considered statistically significant.

Results

Clinicopathological features and HRD status of NSCLC patients

Among the 355 enrolled treatment-naïve NSCLC patients,

there were 229 (64.5%) males and 126 (35.5%) females, with a median age of 68.0 years. Of these, 218 (61.4%) patients were in stage IIIb–IV, 251 (70.7%) had adenocarcinoma, and 163 (45.9%) had a history of smoking. Driver gene variations were present in more than 208 (58.6%) patients (Table 1), including 134 (37.7%) with *EGFR* variations and 12 (3.4%) with *ALK* fusion. These clinicopathological and molecular characteristics are consistent with previous reports (1,35–39). Additionally, 236 (66.5%) patients were available for prognostic evaluation, including 89 surgically treated patients with or without adjuvant therapy, and 147 non-surgically treated patients receiving targeted therapy, immunotherapy, and chemotherapy (Figure 1A). Of the samples, 89/355 (25.1%) were identified as HRD-positive, and 266 (74.9%) were

Table 1 Clinicopathological and molecular characteristics

| Characteristics | n (%) | | | P |
|---------------------------|-------------------|---------------------|----------------------|--------|
| | Total (N=355) | HRD-positive (n=89) | HRD-negative (n=266) | |
| Age [median (IQR)] (year) | 68.0 (61.0, 74.0) | 68.0 (61.0, 75.0) | 68.0 (60.8, 74.0) | 0.342 |
| Gender | | | | 0.052 |
| Male | 229 (64.5) | 65 (73.0) | 164 (61.7) | |
| Female | 126 (35.5) | 24 (27.0) | 102 (38.3) | |
| Smoking | | | | 0.022 |
| Yes | 163 (45.9) | 50 (56.2) | 113 (42.5) | |
| No | 185 (52.1) | 37 (41.6) | 148 (55.6) | |
| Unknown | 7 (2.0) | 2 (2.3) | 5 (1.8) | |
| Histopathology | | | | <0.001 |
| Adenocarcinoma | 251 (70.7) | 46 (51.7) | 205 (77.1) | |
| Squamous carcinoma | 73 (20.6) | 36 (40.4) | 37(13.9) | |
| Others | 31 (8.7) | 7 (7.9) | 24 (9.0) | |
| Clinical stage | | | | 0.175 |
| Ia–IIIa | 133 (37.5) | 28 (31.5) | 105 (39.5) | |
| IIIb–IV | 218 (61.4) | 60 (67.4) | 158 (59.4) | |
| Unknown | 4 (1.1) | 1 (1.1) | 3 (1.1) | |
| Family history | | | | 0.543 |
| Yes | 49 (13.8) | 14 (15.7) | 35 (13.2) | |
| No | 306 (86.2) | 75 (84.3) | 231 (86.8) | |
| Driver genes mutation† | | | | <0.001 |
| Yes | 208 (58.6) | 36 (40.4) | 172 (64.7) | |
| No | 147 (41.4) | 53 (59.6) | 94 (35.3) | |
| TMB status | | | | <0.001 |
| TMB-H (≥ 10 Mut/Mb) | 92 (25.9) | 36 (40.4) | 56 (21.1) | |
| TMB-L (< 10 Mut/Mb) | 263 (74.1) | 53 (59.6) | 210 (78.9) | |

†, Driver genes mutations: *EGFR* exon 18–21, *KRAS* exon 2, *BRAF*^{V600}, *ERBB2* (*HER2*) 20ins, *MET* exon 14 skipping, *RET/ROS1/ALK* fusions. IQR, interquartile range; TMB, tumor mutation burden; HRD, homologous recombination deficiency.

HRD-negative (Figure 1B).

Compared to HRD-negative patients, a higher proportion of HRD-positive NSCLC patients had a history of smoking (56.2% vs. 41.6%, $P=0.022$), fewer had adenocarcinoma (51.7% vs. 77.1%, $P<0.001$), and more had squamous cell carcinoma or other histological types (48.3% vs. 22.9%, $P<0.001$). However, there were no significant differences in age, gender, family history of tumors and clinical stage (Table 1).

Prognosis of NSCLC patients with different HRD status

Among the 147 patients who received non-surgical treatments, 44 were HRD-positive, and 103 were HRD-negative. The PFS of HRD-positive patients was significantly shorter than that of HRD-negative patients [median PFS: 12 vs. 16 months, hazard ratio (HR) (95% CI): 0.53 (0.28–0.98), $P=0.047$, Figure 2A], indicating that HRD-positive NSCLC patients have a poorer overall prognosis. In this group, 20 HRD-positive and 71 HRD-negative patients received targeted therapy. Similarly, the PFS of HRD-positive patients was shorter than that of HRD-negative patients [median PFS: 12 vs. 16 months, HR (95% CI): 0.43 (0.18–0.99), $P=0.042$, Figure 2B], suggesting that HRD-positive NSCLC patients with driver gene mutations do not respond well to targeted therapy. Further analysis of patients receiving first- or third-generation EGFR-TKI therapy showed that EGFR-mutated, HRD-positive NSCLC did not respond well to either generation of TKI [median PFS, HRD-positive, first-TKI vs. HRD-positive, third-TKI: 7 vs. 12 months, HR (95% CI): 0.33 (0.04–3.09), $P=0.331$]. Additionally, the survival of HRD-positive patients was not as good as that of HRD-negative patients receiving third-generation TKI therapy [median PFS, HRD-positive, third-TKI vs. HRD-negative, third-TKI: 12 months vs. not reached, HR (95% CI): 0.21 (0.05–0.96), $P=0.043$] (Figure 2C). However, compared to first-generation TKI, third-generation TKI showed improved efficacy in HRD-positive patients, suggesting these patients may benefit from treatment with third-generation TKI.

For patients without EGFR and MET variants who received immunotherapy, HRD-positive patients showed a numerically poorer response to platinum-free immune combination regimens [median PFS, HRD-positive, Plt- vs. HRD-positive, Plt+: 5.0 vs. 18.0 months, HR (95% CI): 0.28 (0.06–1.44), $P=0.129$, Figure 2D]. Additionally, we analyzed treatment and prognosis information for 89

patients with perioperative treatment, including 11 HRD-positive and 78 HRD-negative patients. No significant difference in DFS was observed between HRD-positive and HRD-negative patients (Supplementary Figure S1).

Prognosis related genomic characterization of NSCLC patients with different HRD status

The relationship between gene alterations and different HRD statuses was shown in the mutational landscape of the NSCLC patients (Figure 3A). According to SNV percentage analysis, the mutation frequency of several genes such as TP53 (89% vs. 56%), NOTCH3 (11% vs. 3%), BRCA1 (4% vs. 1%), BRCA2 (9% vs. 3%), MYC (3% vs. 0%), PRKDC (4% vs. 1%), and CREBBP (9% vs. 3%) was significantly higher in HRD-positive patients than in HRD-negative patients (Figure 3A,B). HRD-positive patients were more susceptible to PIK3CA (18% vs. 3%), MYC (17% vs. 6%), MET (13% vs. 6%), RICTOR (10% vs. 4%), AURKA (6% vs. 2%), and TOP2A (6% vs. 0) CNV amplification (Figure 3A,C). Compared to HRD-negative patients, the frequency of tumor driver genes was lower (40.4% vs. 64.3%, $P<0.001$) in HRD-positive patients (Table 1). Additionally, HRD-positive patients had higher median TMB values (7.50 Mut/Mb vs. 3.84 Mut/Mb, $P<0.001$, Figure 3E, Supplementary Figure S2) and a higher proportion of TMB-H status (≥ 10 Mut/Mb, 40.4% vs. 21.1%, $P<0.001$, Table 1) than HRD-negative patients.

In this cohort, 120 (33.8%) patients carried a total of 170 HRR-related gene mutations. Among these, FANCA (23/355, 6.5%) was the most mutated HRR-related gene, followed by ATM (22/355, 6.2%), BRCA2 (21/355, 5.9%), ATR (19/355, 5.4%), CDK12 (10/355, 2.8%) and BRIP1 (10/355, 2.8%) (Supplementary Table S1). In HRD-positive patients, 15.7% (14/89) carried deleterious mutations in HRR-related genes, significantly higher than in HRD-negative patients (6.4%, 17/266, $P=0.007$). These deleterious mutations were mainly somatic in both HRD-positive (13/14) and HRD-negative patients (12/117), but the frequency of somatic deleterious mutations in HRR-related genes was higher in HRD-positive patients (14.6%, 13/89 vs. 4.5%, 12/266, $P=0.001$, Supplementary Table S2). Among the 120 patients with HRR-related gene mutations, 31 patients carried deleterious mutations. This included 25 cases with 28 somatic mutations (3 carried 2 somatic deleterious mutations) in 12 genes: BRCA2, ATM, ATR, FANCA, BRCA1, CHEK1, CHEK2, BARD1, BRIP1, CDK12, RAD51C, and RAD54L, and 6 cases with 6 germline

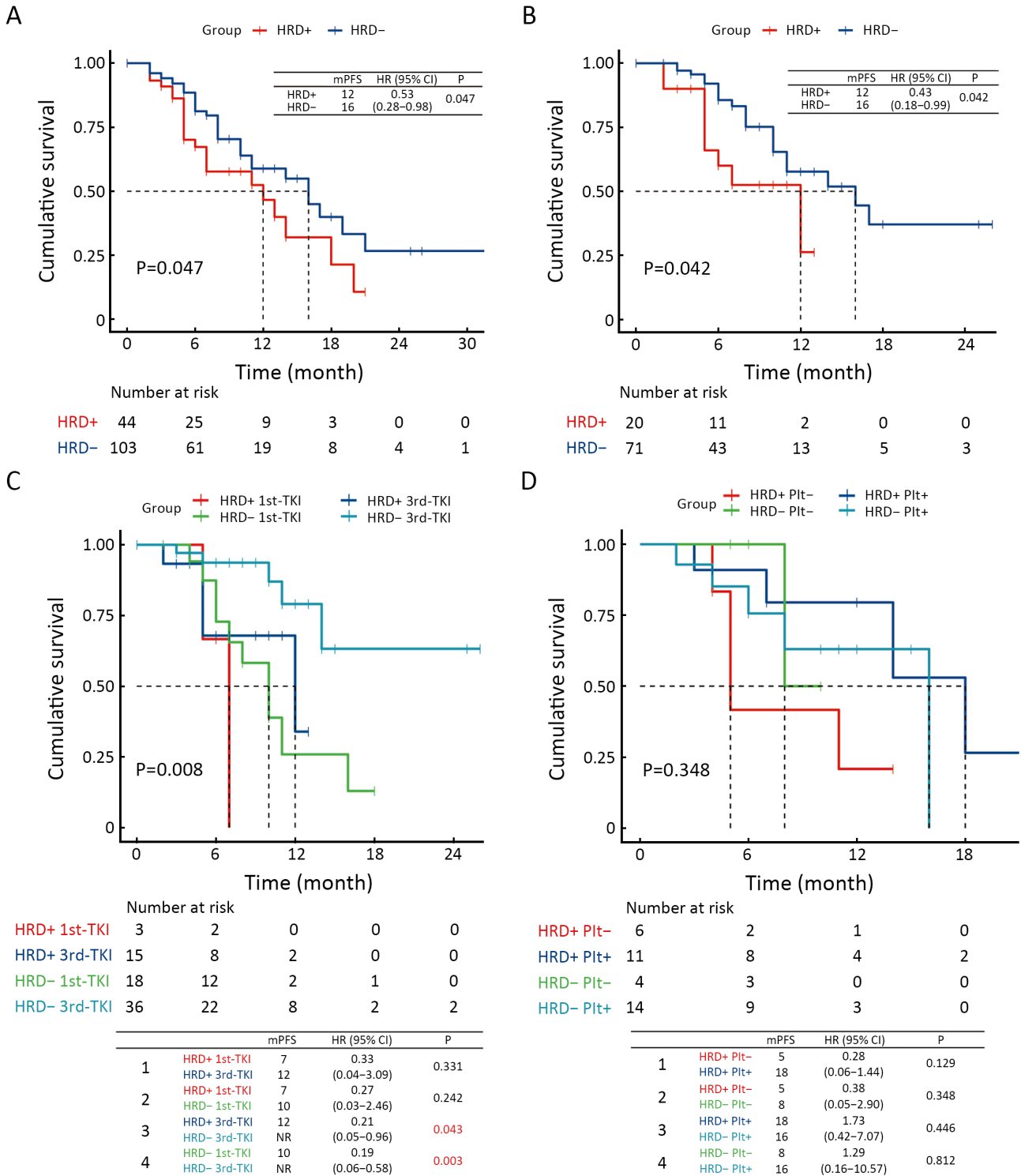


Figure 2 Prognosis of NSCLC patients in different subgroups. (A) Kaplan-Meier plot showed PFS of all patients with different HRD status; (B) PFS of the patients with different HRD status who received targeted therapy; (C) PFS of the patients with different HRD status who received either first- or third-generation TKI; (D) PFS of the patients with different HRD status who received either Plt- immune regimens or Plt+ and immune combination regimens. NSCLC, non-small cell lung cancer; PFS, progression-free survival; HRD, homologous recombination defect; Plt-, platinum-free; Plt+, platinum.

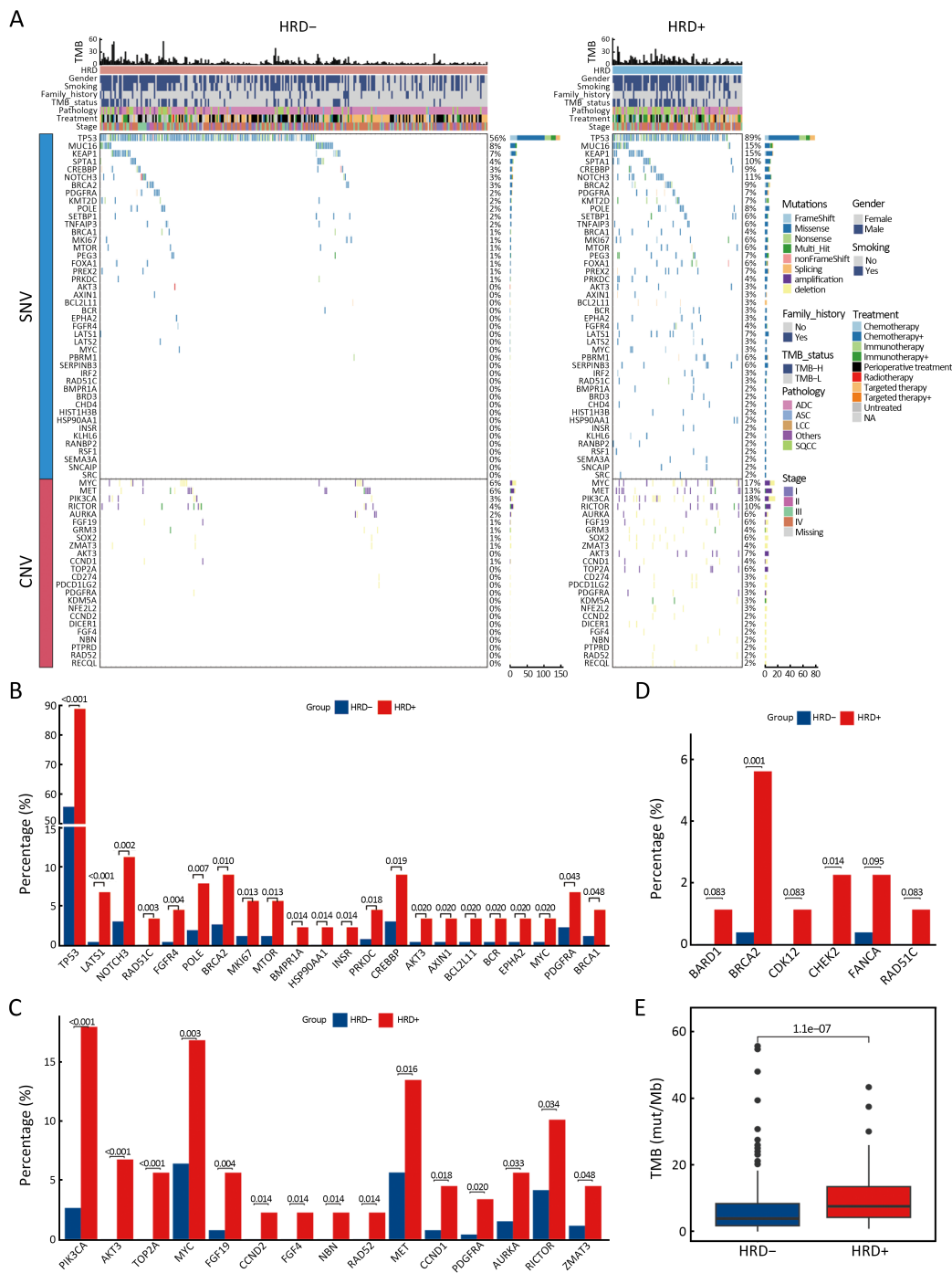


Figure 3 Difference of gene variations between HRD- and HRD+ NSCLC patients. (A) Mutational landscape of all different alterations between HRD- (n=266) and HRD+ (n=89) patients. Upper, TMB values and clinical characteristics, middle, patterns of all gene alterations based on their SNVs, lower, patterns of all gene alterations based on their CNVs. Genes are indicated on the left and their alteration frequency on the right; (B) The most significant different (P<0.05) gene alterations based on SNVs, which enriched in Hallmark pathways; (C) The most significant different (P<0.05) gene alterations based on CNVs, which enriched in Hallmark pathways; (D) Different HRR-related somatic mutations (P<0.1) between HRD+ and HRD- patients; (E) Difference of TMB values between HRD- and HRD+ patients. HRD-, HRD-negative; HRD+, HRD-positive; HRD, homologous recombination defect; NSCLC, non-small cell lung cancer; TMB, tumor mutation burden; SNV, single nucleotide variation; CNV, copy number variation; HRR, homologous recombination repair.

mutations in 5 genes: *ATM*, *BARD1*, *BRCA2*, *RAD51D*, and *FANCA* (Supplementary Table S3). We found that patients with *BRCA2* (P=0.001) and *CHEK2* (P=0.014) somatic mutations were significantly more likely to be HRD-positive than HRD-negative (Figure 3D).

Characterization of CNV and oncogenic pathways in HRD-positive NSCLC patients with different mutation status of driver genes (*EGFR* or *ALK*)

Considering the influence of driver gene on prognosis of patients, we further analyzed feature of CNV and oncogenic pathways in HRD-positive NSCLC patients with different *EGFR* or *ALK* mutant status. Patients with *EGFR* or *ALK* mutations and *EGFR* or *ALK* wild-type were divided into two groups, respectively, according to their HRD status. There were 20 HRD-positive and 40 HRD-negative patients in *EGFR* or *ALK* mutations group and 19 HRD-positive patients and 46 HRD-negative patients in *EGFR* or *ALK* wild-type group. As shown in Figure 4A, in patients with *EGFR* or *ALK* mutations, compared to HRD-negative patients, HRD-positive NSCLC patients harbored more CNV amplifications such as *MET* (18% vs. 5%, P=0.017), *MYC* (21% vs. 7%, P=0.017), *CDK6* (12% vs. 2%, P=0.008), and *AKT3* (9% vs. 0, P=0.001). Further analysis of these genes significantly altered in HRD-positive patients showed that they were mainly enriched in PI3K-AKT signaling, cell cycle, HR and WNT- β -CATENIN signaling pathways (Figure 4A).

In patients with wild-type *EGFR* or *ALK*, more amplifications occurred in PI3K pathway-related genes, such as *PIK3CA* (27% vs. 4%, P<0.001) and *AKT3* (5% vs. 0, P=0.004), as well as cell proliferation-related genes, such as *AURKA* (5% vs. 0, P=0.004) and *TOP2A* (5% vs. 0, P=0.004) (Figure 4B, Supplementary Figure S3). Additionally, in *EGFR* or *ALK* wild-type, HRD-positive patients, altered genes, including CNV and SNV, were significantly enriched in oncogenic pathways like the G2M checkpoint, mitotic spindle, apoptosis, P53 pathway, NOTCH signaling, and WNT- β -CATENIN signaling pathways (Figure 4B).

Tumor microenvironmental characterization of HRD-positive NSCLC patients with different mutation status of driver genes (*EGFR* or *ALK*)

Differences in gene expression (Supplementary Figure S4) and the TME between HRD-positive and HRD-negative patients were analyzed for both *EGFR* or *ALK* mutations

and wild-type statuses. In patients with *EGFR* or *ALK* mutations, pathways significantly enriched in HRD-positive patients were mostly related to cell proliferation, while anti-tumor immunity pathways were enriched in HRD-negative patients (Figure 5A). Additionally, HRD-positive and HRD-negative patients had distinct TME phenotypes. HRD-positive patients showed high enrichment in tumor proliferation and helper immune characteristics, such as “tumor proliferation rate” and “type 2 T helper cell”. In contrast, HRD-negative patients were enriched in anti-tumor immunity characteristics, such as “MHC II” and “effector memory CD8 T cell” (Figure 5C). Similar results were observed in patients with wild-type *EGFR* or *ALK*. Cell proliferation-related pathways were significantly enriched in HRD-positive patients, while anti-tumor immunity pathways were enriched in HRD-negative patients (Figure 5B). HRD-positive patients with wild-type *EGFR* or *ALK* displayed an immunosuppressive TME (Figure 5D). These findings suggest that, regardless of driver gene (*EGFR* or *ALK*) mutation status, HRD-positive NSCLC patients highly expressed genes associated with cell cycle and PI3K-related pathways, and their TME showed immunosuppression and high Th2 cell infiltration.

Genes involved in immune checkpoint and IFN- γ signaling pathways were also investigated in HRD-positive and HRD-negative patients with different driver gene (*EGFR* or *ALK*) statuses. No significant difference in immune checkpoint genes was observed between HRD-positive and HRD-negative patients with *EGFR* or *ALK* mutations (Figure 5E, Supplementary Figure S5A). The expression of IFN- γ genes, including *CIITA*, *CCL5* and *HLA-DRA*, was significantly higher in HRD-negative patients than in HRD-positive patients (P<0.05, Figure 5E, Supplementary Figure S5C). In patients with wild-type *EGFR* or *ALK*, compared to HRD-positive patients, HRD-negative NSCLC patients had higher expression of *HAVCR2*, *PDCD1LG2* and *VSIR* in immune checkpoint genes and *CIITA*, *HLA-E*, *HLA-DRA*, *CCL5*, *CXCL10*, *CD2*, *CD3E*, *GZMK* and *GZMB* in IFN- γ genes (P<0.05, Figure 5F, Supplementary Figure S5B,D).

Discussion

As a hallmark of malignant tumors, HRD and its clinical relevance have been well established in breast, ovarian, prostate and pancreatic cancers (9,10). However, the clinical relevance of HRD in NSCLC, especially in untreated, advanced cases, has not been fully investigated.

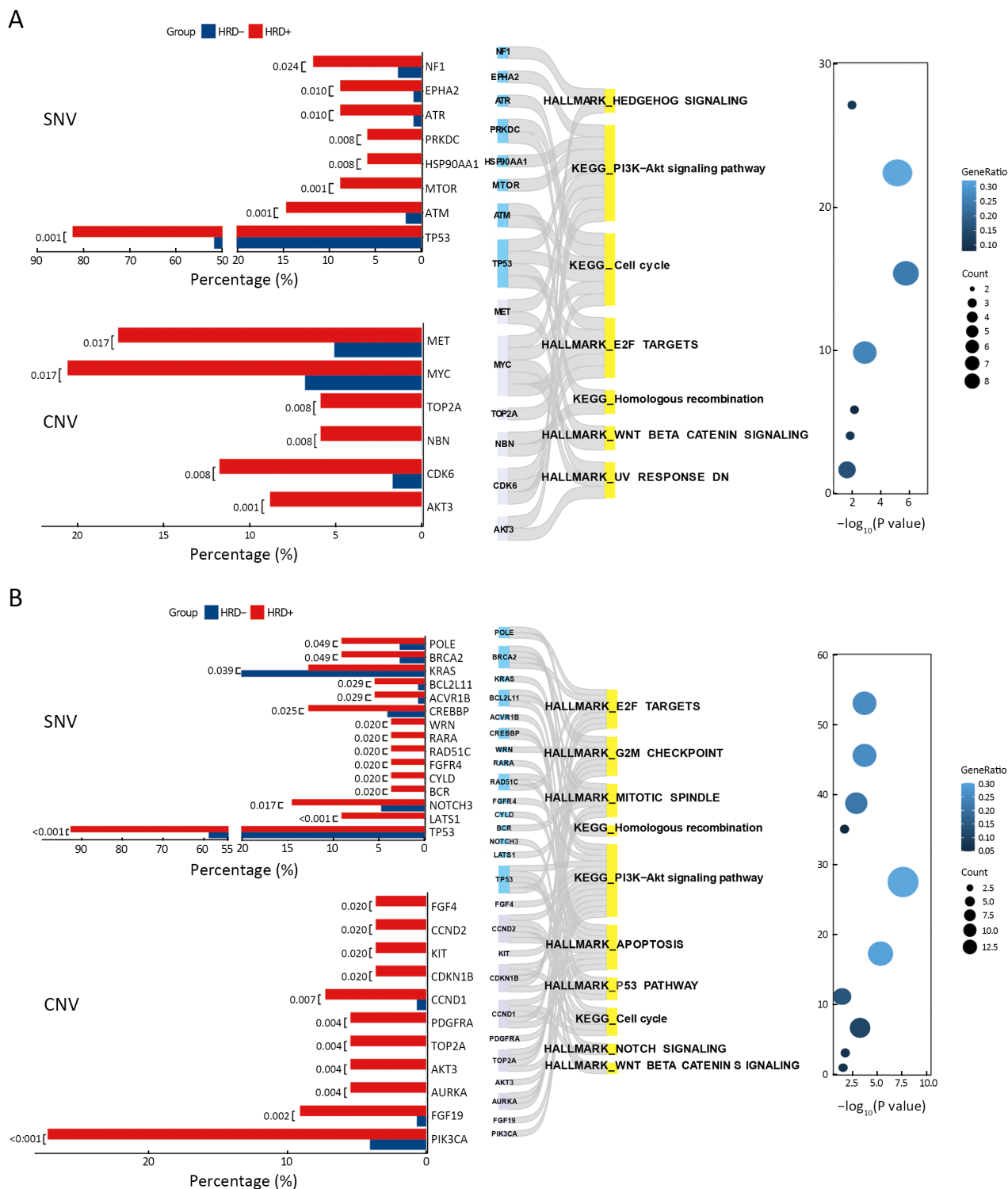


Figure 4 Difference of gene variations between HRD+ and HRD- NSCLC patients with/without *EGFR* or *ALK* mutation. (A) The most significant different ($P < 0.05$) gene alterations between HRD+ and HRD- patients with mutant *EGFR* or *ALK*; (B) The most significant different ($P < 0.05$) gene alterations between HRD+ and HRD- patients with wide-type *EGFR* or *ALK*. HRD-, HRD-negative; HRD+, HRD-positive; HRD, homologous recombination defect; NSCLC, non-small cell lung cancer; *EGFR*, epidermal growth factor receptor; *ALK*, anaplastic lymphoma kinase; KEGG, Kyoto Encyclopedia of Genes and Genomes.

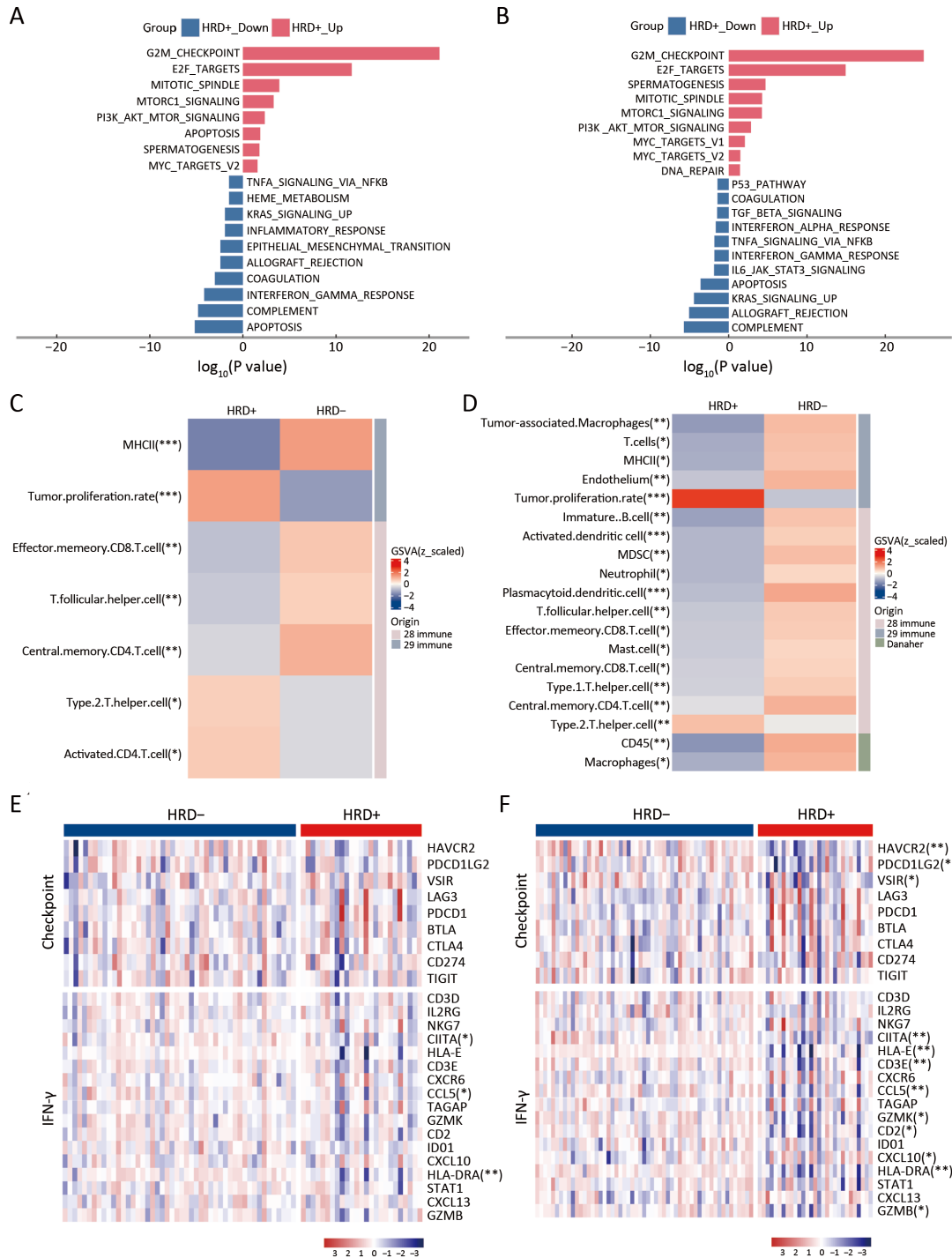


Figure 5 TME of different HRD status NSCLC patients with/without *EGFR* or *ALK* mutation. Important hallmark pathways between HRD- and HRD+ NSCLC patients with mutant *EGFR* or *ALK* (A) or with wide-type *EGFR* or *ALK* (B). Immune signatures from 28 immune sets, 29 immune sets, and cibersort with significant differences between HRD- and HRD+ NSCLC patients with mutant *EGFR* or *ALK* (C) or with wide-type *EGFR* or *ALK* (D). Immune checkpoint and IFN- γ pathway genes between HRD- and HRD+ NSCLC patients with mutant *EGFR* or *ALK* (E) or with wide-type *EGFR* or *ALK* (F). TME, tumor microenvironment; HRD, homologous recombination defect; HRD-, HRD-negative; HRD+, HRD-positive; NSCLC, non-small cell lung cancer; *EGFR*, epidermal growth factor receptor; *ALK*, anaplastic lymphoma kinase. *, P<0.05; **, P<0.01; ***, P<0.001.

This study examined the clinicopathological and prognostic significance of HRD, as well as the biological implications of genomic, transcriptomic and microenvironmental factors associated with prognosis in 355 untreated NSCLC patients. The impact of HRD on the efficacy of targeted therapy and immunotherapy in advanced/metastatic NSCLC was also explored. To date, our study explained the prognosis of advanced HRD NSCLC based on molecular and microenvironmental features.

We found that HRD-positive NSCLC patients might have a poorer prognosis. Consistent with previous studies indicating an approximately 30% HRD-positive rate in NSCLC (51% in lung squamous carcinoma and 35.8% in lung adenocarcinoma) (15), 25.1% (89/355) of the untreated NSCLC patients in this study were HRD-positive. In untreated NSCLC patients, males, ever-smokers, and patients with squamous cell carcinoma had a higher proportion of HRD positivity, aligning with factors reported in previous studies (16,40). Additionally, it is reported that more HRD-positive cases in advanced disease stages reflect the role of chromosomal and genomic instability in driving tumor progression (41-44). However, we did not find a significant difference in the proportion of HRD-positive treatment-naïve NSCLC cases between operable and advanced patients in our study.

We further subdivided the drug therapy categories and found that HRD-positive NSCLC patients had a worse response to targeted therapy compared to HRD-negative patients, with significant differences observed. HRD-positive patients responded poorly to both first- and third-generation EGFR-TKIs, but the third-generation EGFR-TKI showed improved efficacy compared to the first-generation TKIs in HRD-positive patients. Previous studies have shown that the efficacy of EGFR- or ALK-TKIs can be poor in combination with *TP53* mutations and other tumor suppressor genes (45,46). Our data revealed that 89% of HRD-positive patients carry *TP53* mutations, suggesting that HRD affects the efficacy of targeted therapy and may be a better indicator for the diverse efficiency of NSCLC patients with *EGFR* mutations. Additionally, to explore the molecular characteristics influencing patient prognosis, we performed a complementary analysis using the Benjamini-Hochberg (BH) method to adjust for multiple comparisons of SNV/CNV alterations and gene expression between different HRD states (*Supplementary Tables S4–15*). This study focuses on effector molecules that show both statistically significant P values and biological significance,

reducing the risk of highlighting false positives based on statistical significance alone. Our findings are supported by previous reports. Specifically, Talia *et al.* identified a significant prevalence of mutations in *BRCA1/2*, *PALB2*, *RAD51C/D* and *XRCC2* among patients with HRD-positive pancreatic ductal adenocarcinoma (PDAC) (47). Alterations in *TP53* were confirmed to be enriched in HRD-positive ovarian cancer (48). *MYC* amplification was found to be increased in HRD-positive breast cancer (49).

HRD-positive NSCLC displayed a higher frequency of copy-number amplification in well-known oncogenes such as *MET* and *PIK3CA*. Transcriptionally, pathways related to the cell cycle and RTK were enriched in HRD-positive NSCLC. These molecular features may contribute to resistance to targeted therapy in driver-positive NSCLC. Additionally, similar HRD-related genomic features, such as fewer mutated driver genes, a higher frequency of *TP53* and HRR mutations, and elevated TMB, were also found in HRD-positive NSCLC (17,50). The inability of HRD to repair double-strand breaks may trigger genomic instability (GIN), which can contribute to the development and drug resistance of malignant tumors (41-43). Copy number alterations occur more easily in GIN cancers. In this study, HRD-positive NSCLC showed more CNV events, especially amplifications of oncogenes. Although differed, it was clinically relevant CNV spectrum was identified in HRD-positive NSCLC with or without *EGFR* or *ALK* mutations. The poor response to EGFR-TKI therapy in HRD-positive patients with *EGFR* or *ALK* mutations may also be due to the coexistence of HRD and gene amplifications, or the combination of HRD and gene amplification leading to TKI resistance. Additionally, amplification of the *MET* gene was more common in the HRD-positive NSCLC group with *EGFR* or *ALK* driver mutations, which may mediate intrinsic resistance to EGFR- and ALK-TKIs (51). Therefore, it is important to consider the possible association of *MET* amplification with intrinsic resistance mechanisms to EGFR- or ALK-TKIs.

In this study, HRD-positive patients with *EGFR* and *MET* wild-type NSCLC who received a platinum-free chemoimmunotherapy regimen showed shorter median PFS. In contrast, HRD-negative NSCLC patients showed no difference in efficacy between platinum-containing and platinum-free regimens. Despite the higher proportion of TMB-H in HRD-positive patients, the efficacy of immunotherapy in these patients was inconsistent with previous studies (17,21). This inconsistency may be due to the lack of homozygosity leading to genomic instability,

resulting in more DNA damage and elevated TMB (50). Genomic instability may also lead to intra-tumoral heterogeneity (42), which can present as elevated TMB (44). Currently, no definitive data exist on the predictive effect of HRD status in immunotherapy combined with chemotherapy, as studies, including this one, have been conducted in different disease stages. The tumor microenvironment in early or late disease stages may influence the therapeutic efficacy of immunotherapy. Additionally, as NSCLC progresses, the continuous accumulation of CNVs in pro-tumoral genes may further suppress anti-tumor immunity while enhancing immune suppression and the mesenchymal phenotype of the TME (52-56). Thus, HRD status may have bipolar effects on early and late stages of NSCLC.

In our study, the amplification of genes in the PI3K pathway (*PIK3CA* and *AKT3*) and cell cycle-related genes (*AURKA*, *TOP2A*, *SOX2*, and *CCND1*) was more common in *EGFR* or *ALK* wild-type, HRD-positive NSCLC. Activation of the PI3K/AKT pathway and the cell cycle may drive cancer development (57). As previously reported (58), CNVs in genes within these pathways may contribute to an immunosuppressive microenvironment, potentially reducing the efficacy of immunotherapy (57). Consistent with the genomic findings in HRD-positive NSCLC, transcriptomic data also indicated that tumor proliferation and an immunosuppressive microenvironment were highly enriched in the HRD-positive group. HRD-negative patients, on the other hand, showed enrichment in anti-tumor immunity characteristics, such as “MHC II” and “effector memory CD8 T cell”. This finding aligns with TCGA data from pan-cancer analyses. The HRD sum score and the T-cell inflamed gene expression profile correlated weakly in lung adenocarcinoma and squamous cell carcinoma (59). Recent advances have highlighted the importance of the tumor immune microenvironment in determining the clinical response to immunotherapy in lung cancer (60,61).

The results of our microenvironment analysis align with the prognosis of immunotherapy in this study, prompting NSCLC patients with HRD-positive status may apply platinum agents in immunotherapy to increase clinical benefits. Although HRD could be a prognostic biomarker for immunotherapy, more studies are needed to verify the correlation between HRD status and immunotherapy efficiency. In addition, a combination therapeutic strategy should be suggested and validated in HRD-positive NSCLC patients (62), such as using PARPi or platinum

combined with immunotherapy.

Several limitations of this study should be discussed. First, the molecular classification based on HRD status may have potential clinical value for prognosis and therapy choices, but it is not fully verified due to the retrospective nature of the data. Future multi-center, prospective studies are needed to further verify the clinical value of HRD-positive status in NSCLC. Second, untreated patients were enrolled in this study, but the difference in HRD-positive value between treatment-naïve and treated NSCLC, and the existence of acquired HRD-positive status, is still under investigation. Third, a pre-defined cut-off value (≥ 50) for HRD positivity was used in this study. An NSCLC-specific HRD cut-off should be established and validated in future research.

Conclusions

This study revealed for the first time the unique clinical pathology, genomic characteristics, expression profiles and microenvironment features of untreated HRD-positive NSCLC patients. We found that HRD-positive patients have a poor prognosis and a reduced response to EGFR-TKI treatment and platinum-free chemotherapy combined with immunotherapy. Given the mutation characteristics of HRD-positive patients, PARPi or combining with drugs targeting *PIK3CA*, *MET*, *MYC* and other mutations may be viable treatment options. Our study highlights potential actionable alterations in HRD-positive NSCLC, suggesting possible combinational therapeutic strategies for these patients (63-65).

Acknowledgements

This study was supported by the National High Level Hospital Clinical Research Funding (No. BJ-2219-195 and No. BJ-2023-090).

Footnote

Conflicts of Interest: The authors have no conflicts of interest to declare.

References

- Herbst RS, Morgensztern D, Boshoff C. The biology and management of non-small cell lung cancer. *Nature* 2018;553:446-54.

2. National Health Commission of the People's Republic of China. National guidelines for diagnosis and treatment of lung cancer 2022 in China (English version). *Chin J Cancer Res* 2022;34:176-206.
3. Imyanitov EN, Iyevleva AG, Levchenko EV. Molecular testing and targeted therapy for non-small cell lung cancer: Current status and perspectives. *Crit Rev Oncol Hematol* 2021;157:103194.
4. Tan AC, Tan DSW. Targeted therapies for lung cancer patients with oncogenic driver molecular alterations. *J Clin Oncol* 2022;40:611-25.
5. Huang Q, Zhang H, Hai J, et al. Impact of PD-L1 expression, driver mutations and clinical characteristics on survival after anti-PD-1/PD-L1 immunotherapy versus chemotherapy in non-small-cell lung cancer: A meta-analysis of randomized trials. *Oncoimmunology* 2018;7:e1396403.
6. Rossi A, Di Maio M. Platinum-based chemotherapy in advanced non-small-cell lung cancer: optimal number of treatment cycles. *Expert Rev Anticancer Ther* 2016;16:653-60.
7. Melosky B, Wheatley-Price P, Juergens RA, et al. The rapidly evolving landscape of novel targeted therapies in advanced non-small cell lung cancer. *Lung Cancer* 2021;160:136-51.
8. Burgess JT, Rose M, Boucher D, et al. The therapeutic potential of DNA damage repair pathways and genomic stability in lung cancer. *Front Oncol* 2020;10:1256.
9. Abkevich V, Timms KM, Hennessy BT, et al. Patterns of genomic loss of heterozygosity predict homologous recombination repair defects in epithelial ovarian cancer. *Br J Cancer* 2012;107:1776-82.
10. Popova T, Manié E, Rieunier G, et al. Ploidy and large-scale genomic instability consistently identify basal-like breast carcinomas with BRCA1/2 inactivation. *Cancer Res* 2012;72:5454-62.
11. Birkbak NJ, Wang ZC, Kim JY, et al. Telomeric allelic imbalance indicates defective DNA repair and sensitivity to DNA-damaging agents. *Cancer Discov* 2012;2:366-75.
12. Riaz N, Bleuca P, Lim RS, et al. Pan-cancer analysis of bi-allelic alterations in homologous recombination DNA repair genes. *Nat Commun* 2017;8:857.
13. Shim JH, Kim HS, Cha H, et al. HLA-corrected tumor mutation burden and homologous recombination deficiency for the prediction of response to PD-(L)1 blockade in advanced non-small-cell lung cancer patients. *Ann Oncol* 2020;31:902-11.
14. Kadouri L, Rottenberg Y, Zick A, et al. Homologous recombination in lung cancer, germline and somatic mutations, clinical and phenotype characterization. *Lung Cancer* 2019;137:48-51.
15. Rempel E, Kluck K, Beck S, et al. Pan-cancer analysis of genomic scar patterns caused by homologous repair deficiency (HRD). *NPJ Precis Oncol* 2022;6:36.
16. Feng J, Lan Y, Liu F, et al. Combination of genomic instability score and TP53 status for prognosis prediction in lung adenocarcinoma. *NPJ Precis Oncol* 2023;7:110.
17. Zhou Z, Ding Z, Yuan J, et al. Homologous recombination deficiency (HRD) can predict the therapeutic outcomes of immuno-neoadjuvant therapy in NSCLC patients. *J Hematol Oncol* 2022;15:62.
18. Fennell DA, Porter C, Lester J, et al. Olaparib maintenance versus placebo monotherapy in patients with advanced non-small cell lung cancer (PIN): A multicentre, randomised, controlled, phase 2 trial. *EClinicalMedicine* 2022;52:101595.
19. Zhang L, Guan S, Meng F, et al. Next-generation sequencing of homologous recombination genes could predict efficacy of platinum-based chemotherapy in non-small cell lung cancer. *Front Oncol* 2022;12:1035808.
20. Ji W, Weng X, Xu D, et al. Non-small cell lung cancer cells with deficiencies in homologous recombination genes are sensitive to PARP inhibitors. *Biochem Biophys Res Commun* 2020;522:121-6.
21. Shang X, Qi K, Liu X, et al. Signatures associated with homologous recombination deficiency and immune regulation to improve clinical outcomes in patients with lung adenocarcinoma. *Front Oncol* 2022;12:854999.
22. Li S, Hou L, Huang Y, et al. Primary salivary duct carcinoma of the lung: clinicopathological features, diagnosis and practical challenges. *J Clin Pathol* 2024;77:324-9.
23. Chen D, Bao X, Zhang R, et al. Depiction of the genomic and genetic landscape identifies CCL5 as a protective factor in colorectal neuroendocrine carcinoma. *Br J Cancer* 2021;125:994-1002.
24. Richards S, Aziz N, Bale S, et al. Standards and

- guidelines for the interpretation of sequence variants: a joint consensus recommendation of the American College of Medical Genetics and Genomics and the Association for Molecular Pathology. *Genet Med* 2015;17:405-24.
25. Yuan W, Ni J, Wen H, et al. Genomic Scar Score: A robust model predicting homologous recombination deficiency based on genomic instability. *BJOG* 2022;129 Suppl 2:14-22.
 26. Li Y, Ge X, Peng F, et al. Exaggerated false positives by popular differential expression methods when analyzing human population samples. *Genome Biol* 2022;23:79.
 27. Wu T, Hu E, Xu S, et al. clusterProfiler 4. 0: A universal enrichment tool for interpreting omics data. *Innovation (Camb)* 2021;2:100141.
 28. Subramanian A, Tamayo P, Mootha VK, et al. Gene set enrichment analysis: a knowledge-based approach for interpreting genome-wide expression profiles. *Proc Natl Acad Sci U S A* 2005;102:15545-50.
 29. Barbie DA, Tamayo P, Boehm JS, et al. Systematic RNA interference reveals that oncogenic KRAS-driven cancers require TBK1. *Nature* 2009;462:108-12.
 30. Bagaev A, Kotlov N, Nomie K, et al. Conserved pan-cancer microenvironment subtypes predict response to immunotherapy. *Cancer Cell* 2021;39:845-65.e7.
 31. Bindea G, Mlecnik B, Tosolini M, et al. Spatiotemporal dynamics of intratumoral immune cells reveal the immune landscape in human cancer. *Immunity* 2013;39:782-95.
 32. Hänzelmann S, Castelo R, Guinney J. GSEA: gene set variation analysis for microarray and RNA-seq data. *BMC Bioinformatics* 2013;14:7.
 33. Newman AM, Liu CL, Green MR, et al. Robust enumeration of cell subsets from tissue expression profiles. *Nat Methods* 2015;12:453-7.
 34. Becht E, Giraldo NA, Lacroix L, et al. Estimating the population abundance of tissue-infiltrating immune and stromal cell populations using gene expression. *Genome Biol* 2016;17:218.
 35. Socinski MA, Obasaju C, Gandara D, et al. Clinicopathologic features of advanced squamous NSCLC. *J Thorac Oncol* 2016;11:1411-22.
 36. Molina JR, Yang P, Cassivi SD, et al. Non-small cell lung cancer: epidemiology, risk factors, treatment, and survivorship. *Mayo Clin Proc* 2008;83:584-94.
 37. Yang CY, Yang JC, Yang PC. Precision management of advanced non-small cell lung cancer. *Annu Rev Med* 2020;71:117-36.
 38. Harada G, Yang SR, Cocco E, et al. Rare molecular subtypes of lung cancer. *Nat Rev Clin Oncol* 2023;20:229-49.
 39. Teng Y, Xia C, Cao M, et al. Lung cancer burden and trends from 2000 to 2018 in China: Comparison between China and the United States. *Chin J Cancer Res* 2023;35:618-26.
 40. Chen C, Cheng X, Li S, et al. A Novel signature for predicting prognosis of smoking-related squamous cell carcinoma. *Front Genet* 2021;12:666371.
 41. Bakhoun SF, Ngo B, Laughney AM, et al. Chromosomal instability drives metastasis through a cytosolic DNA response. *Nature* 2018;553:467-72.
 42. Bakhoun SF, Landau DA. Chromosomal instability as a driver of tumor heterogeneity and evolution. *Cold Spring Harb Perspect Med* 2017;7:a029611.
 43. Guo S, Zhu X, Huang Z, et al. Genomic instability drives tumorigenesis and metastasis and its implications for cancer therapy. *Biomed Pharmacother* 2023;157:114036.
 44. Weir WH, Mucha PJ, Kim WY. A bipartite graph-based expected networks approach identifies DDR genes not associated with TMB yet predictive of immune checkpoint blockade response. *Cell Rep Med* 2022;3:100602.
 45. Janning M, Süptitz J, Albers-Leischner C, et al. Treatment outcome of atypical EGFR mutations in the German National Network Genomic Medicine Lung Cancer (nNGM). *Ann Oncol* 2022;33:602-15.
 46. Tanimoto A, Matsumoto S, Takeuchi S, et al. Proteasome inhibition overcomes ALK-TKI resistance in *ALK*-rearranged/*TP53*-mutant NSCLC via noxa expression. *Clin Cancer Res* 2021;27:1410-20.
 47. Golan T, O'Kane GM, Denroche RE, et al. Genomic features and classification of homologous recombination deficient pancreatic ductal adenocarcinoma. *Gastroenterology* 2021;160:2119-32.e9.
 48. Wen H, Feng Z, Ma Y, et al. Homologous recombination deficiency in diverse cancer types and its correlation with platinum chemotherapy efficiency in ovarian cancer. *BMC Cancer* 2022;22:550.

49. Jacobson DH, Pan S, Fisher J, et al. Multi-scale characterisation of homologous recombination deficiency in breast cancer. *Genome Med* 2023;15:90.
50. Jiang M, Jia K, Wang L, et al. Alterations of DNA damage response pathway: Biomarker and therapeutic strategy for cancer immunotherapy. *Acta Pharm Sin B* 2021;11:2983-94.
51. Cooper AJ, Sequist LV, Lin JJ. Third-generation EGFR and ALK inhibitors: mechanisms of resistance and management. *Nat Rev Clin Oncol* 2022;19:499-514.
52. Goldmann T, Marwitz S, Nitschkowski D, et al. PD-L1 amplification is associated with an immune cell rich phenotype in squamous cell cancer of the lung. *Cancer Immunol Immunother* 2021;70:2577-87.
53. Griffin GK, Wu J, Iracheta-Vellve A, et al. Epigenetic silencing by SETDB1 suppresses tumour intrinsic immunogenicity. *Nature* 2021;595:309-14.
54. Ravi A, Hellmann MD, Arniella MB, et al. Genomic and transcriptomic analysis of checkpoint blockade response in advanced non-small cell lung cancer. *Nat Genet* 2023;55:807-19.
55. Yoshimura K, Inoue Y, Tsuchiya K, et al. Elucidation of the relationships of MET protein expression and gene copy number status with PD-L1 expression and the immune microenvironment in non-small cell lung cancer. *Lung Cancer* 2020;141:21-31.
56. Zhang XC, Wang J, Shao GG, et al. Comprehensive genomic and immunological characterization of Chinese non-small cell lung cancer patients. *Nature Commun* 2019;10:1772.
57. Sun C, Fang Y, Labrie M, et al. Systems approach to rational combination therapy: PARP inhibitors. *Biochem Soc Trans* 2020;48:1101-8.
58. Ren C, Li J, Zhou Y, et al. Typical tumor immune microenvironment status determine prognosis in lung adenocarcinoma. *Transl Oncol* 2022;18:101367.
59. Budczies J, Kluck K, Beck S, et al. Homologous recombination deficiency is inversely correlated with microsatellite instability and identifies immunologically cold tumors in most cancer types. *J Pathol Clin Res* 2022;8:371-82.
60. Su D, Wu G, Xiong R, et al. Tumor immune microenvironment characteristics and their prognostic value in non-small-cell lung cancer. *Front Oncol* 2021;11:634059.
61. Tie Y, Tang F, Wei YQ, et al. Immunosuppressive cells in cancer: mechanisms and potential therapeutic targets. *J Hematol Oncol* 2022;15:61.
62. Wang Q, Yang S, Wang K, et al. MET inhibitors for targeted therapy of EGFR TKI-resistant lung cancer. *J Hematol Oncol* 2019;12:63.
63. Belli C, Repetto M, Anand S, et al. The emerging role of PI3K inhibitors for solid tumour treatment and beyond. *Br J Cancer* 2023;128:2150-62.
64. Massó-Vallés D, Beaulieu ME, Soucek L. MYC, MYCL, and MYCN as therapeutic targets in lung cancer. *Expert Opin Ther Targets* 2020;24:101-14.
65. Du R, Huang C, Liu K, et al. Targeting AURKA in cancer: molecular mechanisms and opportunities for cancer therapy. *Mol Cancer* 2021;20:15.

Cite this article as: Wang Y, Ma Y, He L, Du J, Li X, Jiao P, Wu X, Xu X, Zhou W, Yang L, Di J, Zhu C, Xu L, Sun T, Li L, Liu D, Wang Z. Clinical and molecular significance of homologous recombination deficiency positive non-small cell lung cancer in Chinese population: An integrated genomic and transcriptional analysis. *Chin J Cancer Res* 2024;36(3):282-297. doi: 10.21147/j.issn.1000-9604.2024.03.05

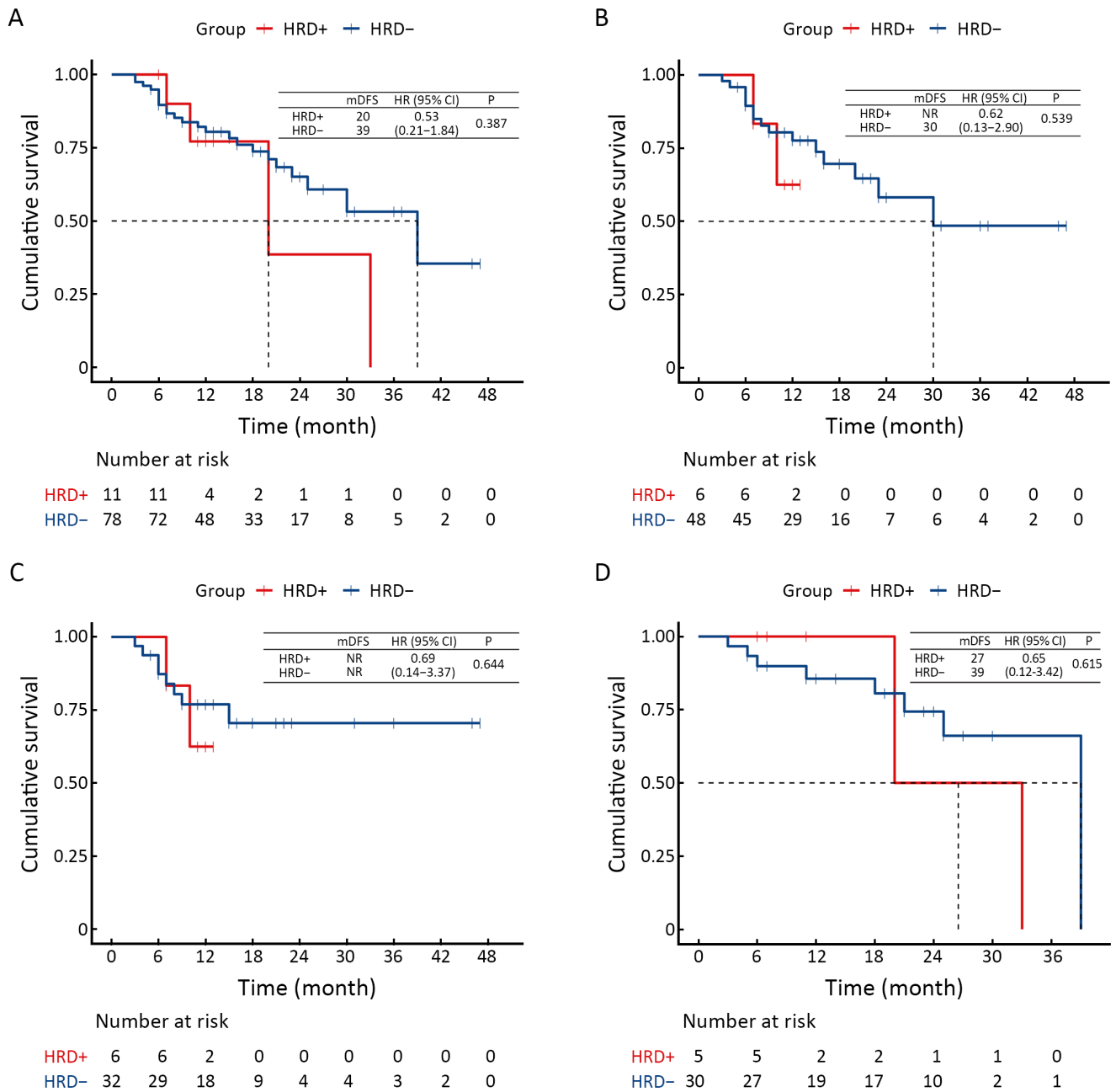


Figure S1 DFS of difference in different subgroups. (A) All patients with different HRD status; (B) Patients with different HRD status who received adjuvant therapy after surgery; (C) Patients with different HRD status who received adjuvant therapy with platinum after surgery; (D) Patients with different HRD status who not received adjuvant therapy after surgery. DFS, disease-free survival; HRD, homologous recombination defect.

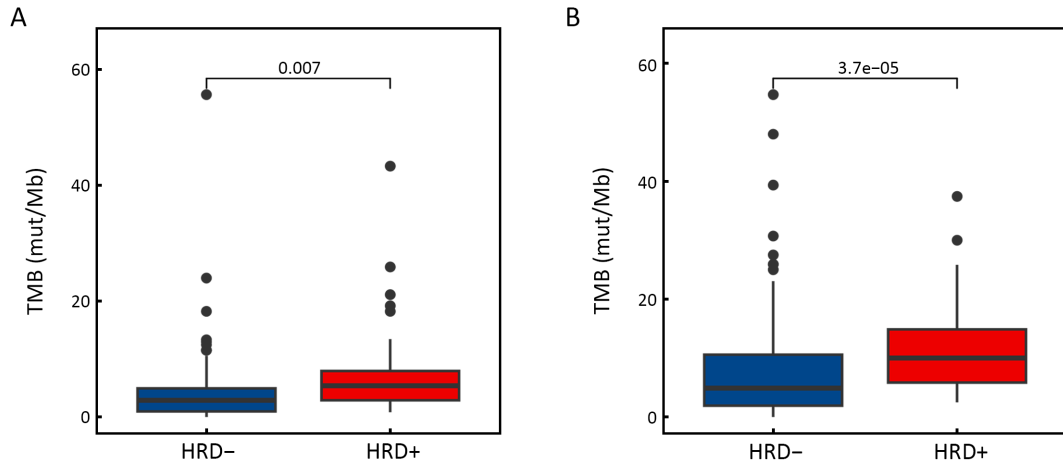


Figure S2 Difference of TMB values between HRD⁻ and HRD⁺ patients with mutant *EGFR* or *ALK* (A) or with wide-type *EGFR* or *ALK* (B). TMB, tumor mutation burden; HRD⁻, HRD-negative; HRD⁺, HRD-positive; HRD, homologous recombination defect; *EGFR*, epidermal growth factor receptor; *ALK*, anaplastic lymphoma kinase.

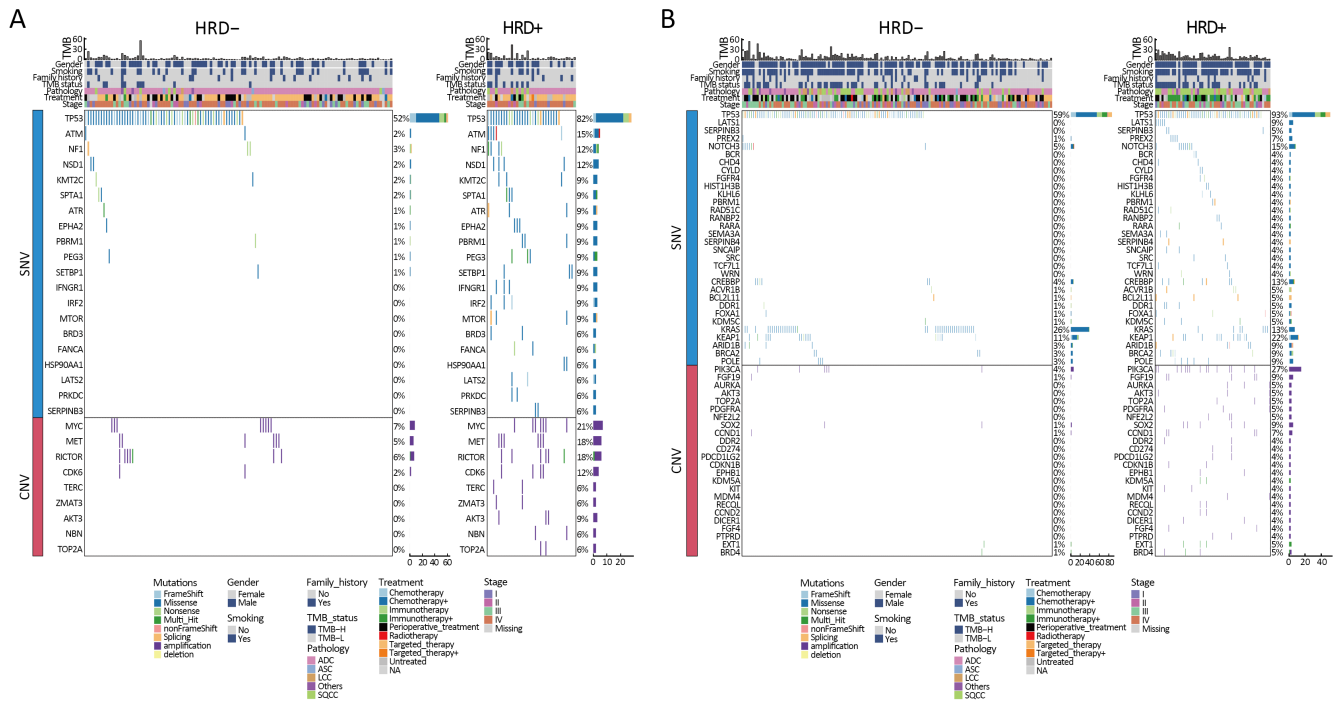


Figure S3 Genetic alterations with significant difference between HRD⁻ and HRD⁺ patients with mutant *EGFR* or *ALK* (A) or with wide-type *EGFR* or *ALK* (B). HRD⁻, HRD-negative; HRD⁺, HRD-positive; HRD, homologous recombination defect; SNV, single nucleotide variation; CNV, copy number variation; *EGFR*, epidermal growth factor receptor; *ALK*, anaplastic lymphoma kinase; TMB, tumor mutation burden.

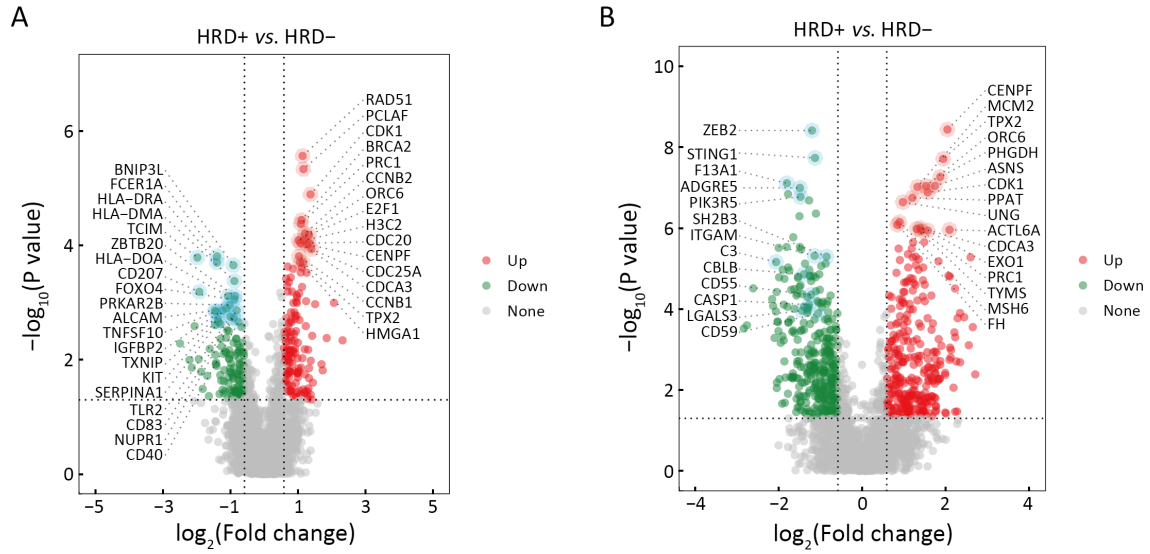


Figure S4 Differential genes volcano map between HRD+ and HRD- patients with mutant *EGFR* or *ALK* (A) or with wide-type *EGFR* or *ALK* (B). Red is HRD+ up-regulated gene, green is HRD+ down-regulated gene. HRD-, HRD-negative; HRD+, HRD-positive; HRD, homologous recombination defect; *EGFR*, epidermal growth factor receptor; *ALK*, anaplastic lymphoma kinase.

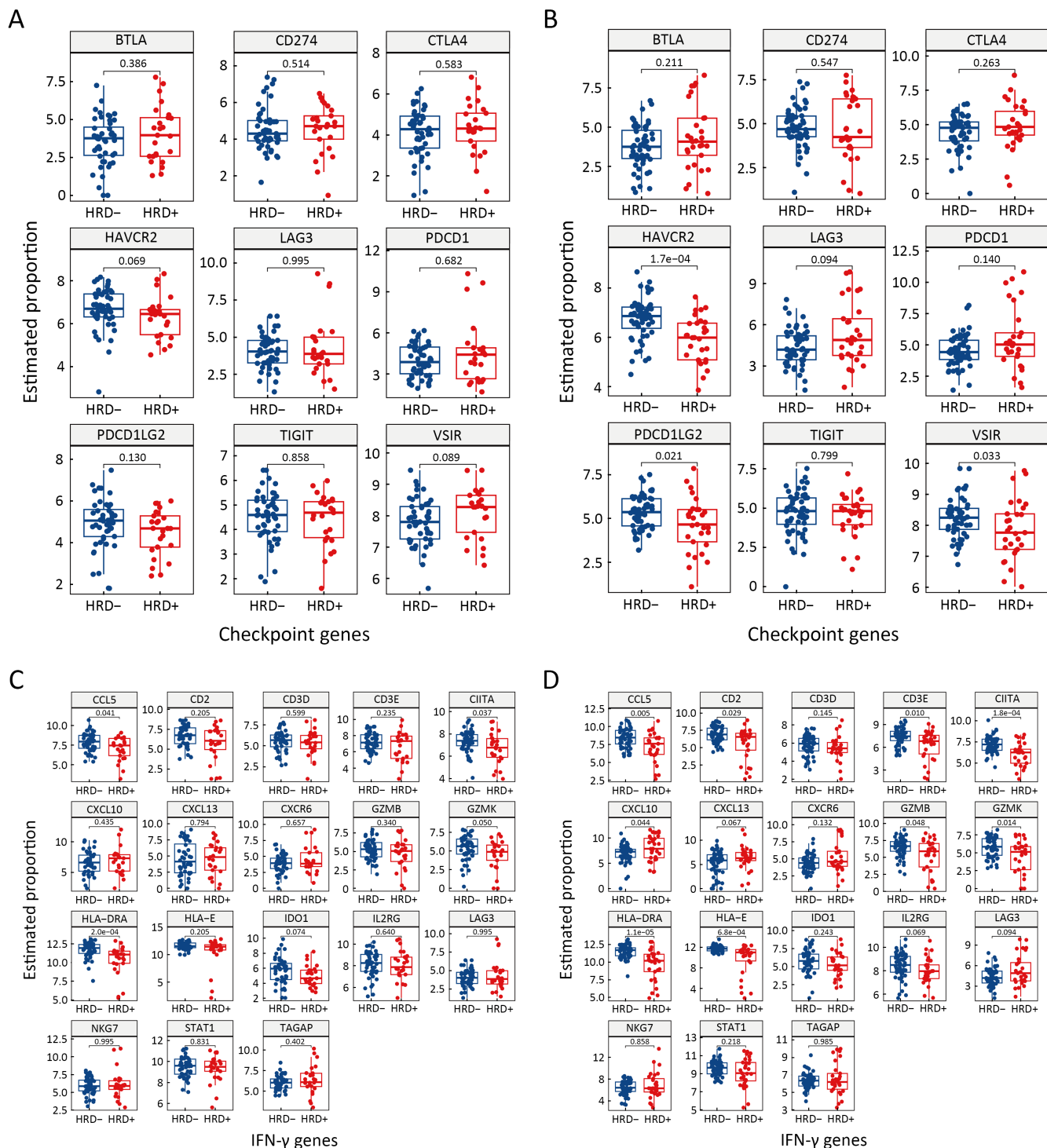


Figure S5 Expression difference of immune checkpoint and IFN- γ genes between HRD+ and HRD- patients with mutant *EGFR/ALK* or with wide-type *EGFR/ALK*. Immune checkpoint genes with mutant *EGFR/ALK* (A) or with wide-type *EGFR/ALK* (B); IFN- γ genes with mutant *EGFR/ALK* (C) or with wide-type *EGFR/ALK* (D). HRD-, HRD-negative; HRD+, HRD-positive; HRD, homologous recombination defect; IFN, interferon; *EGFR*, epidermal growth factor receptor; *ALK*, anaplastic lymphoma kinase.

Table S1 Statistics of HRR mutations loci

| HRR | No. | | | |
|---------------|----------|---------|----------|------------------|
| | Mutation | Somatic | Germline | Somatic+germline |
| <i>ATM</i> | 22 | 16 | 4 | 2 |
| <i>ATR</i> | 19 | 16 | 3 | 0 |
| <i>BARD1</i> | 8 | 4 | 4 | 0 |
| <i>BRCA1</i> | 6 | 5 | 1 | 0 |
| <i>BRCA2</i> | 21 | 15 | 6 | 0 |
| <i>BRIP1</i> | 10 | 10 | 0 | 0 |
| <i>CDK12</i> | 10 | 4 | 6 | 0 |
| <i>CHEK1</i> | 8 | 7 | 1 | 0 |
| <i>CHEK2</i> | 9 | 7 | 2 | 0 |
| <i>FANCA</i> | 23 | 12 | 11 | 0 |
| <i>FANCL</i> | 5 | 3 | 2 | 0 |
| <i>NBN</i> | 9 | 5 | 4 | 0 |
| <i>PALB2</i> | 6 | 4 | 2 | 0 |
| <i>MRE11A</i> | 3 | 3 | 0 | 0 |
| <i>RAD51B</i> | 1 | 0 | 1 | 0 |
| <i>RAD51C</i> | 4 | 3 | 1 | 0 |
| <i>RAD51D</i> | 1 | 0 | 1 | 0 |
| <i>RAD54L</i> | 5 | 1 | 4 | 0 |
| Total | 170 | 115 | 53 | 2 |

HRR, homologous recombination repair.

Table S2 HRR mutation status between HRD-positive and -negative

| Mutation type | n (%) | | P |
|-----------------------------|---------------------|----------------------|-------|
| | HRD-positive (n=89) | HRD-negative (n=266) | |
| HR gene pathogenic mutation | | | 0.007 |
| Yes | 14 (15.7) | 17 (6.4) | |
| No | 75 (84.3) | 249 (93.6) | |
| Germline HR gene mutations | | | 0.632 |
| Yes | 1 (1.1) | 5 (1.9) | |
| No | 88 (98.9) | 261 (98.1) | |
| Somatic HR gene mutations | | | 0.001 |
| Yes | 13 (14.6) | 12 (4.5) | |
| No | 76 (85.4) | 254 (95.5) | |

HRR, homologous recombination repair; HRD, homologous recombination deficiency.

Table S3 Patient statistics of HRR pathogenic mutations

| HRR | No. | | |
|---------------|----------------------|---------|----------|
| | Pathogenic | Somatic | Germline |
| <i>ATM</i> | 7 | 5 | 2 |
| <i>ATR</i> | 3 | 3 | 0 |
| <i>BARD1</i> | 2 | 1 | 1 |
| <i>BRCA1</i> | 2 | 2 | 0 |
| <i>BRCA2</i> | 7 | 6 | 1 |
| <i>BRIP1</i> | 1 | 1 | 0 |
| <i>CDK12</i> | 1 | 1 | 0 |
| <i>CHEK1</i> | 2 | 2 | 0 |
| <i>CHEK2</i> | 2 | 2 | 0 |
| <i>FANCA</i> | 4 | 3 | 1 |
| <i>FANCL</i> | 0 | 0 | 0 |
| <i>NBN</i> | 0 | 0 | 0 |
| <i>PALB2</i> | 0 | 0 | 0 |
| <i>MRE11A</i> | 0 | 0 | 0 |
| <i>RAD51B</i> | 0 | 0 | 0 |
| <i>RAD51C</i> | 1 | 1 | 0 |
| <i>RAD51D</i> | 1 | 0 | 1 |
| <i>RAD54L</i> | 1 | 1 | 0 |
| Total | 34-3=31 [†] | 28 | 6 |

[†], There are three co-mutations between patients. HRR, homologous recombination repair.